

PETROPHYSICAL MEASUREMENTS FOR CO₂ STORAGE: APPLICATION TO THE KETZIN SITE.

M. Fleury¹, S. Gautier¹, N. Gland¹, P. Boulin¹
B. Norden², C. Schmidt-Hattenberger²

(1) IFP, Rueil-Malmaison, France,
(2) GFZ, Potsdam, Germany

This paper was prepared for presentation at the International Symposium of the Society of Core Analysts held in Halifax, Nova Scotia, Canada, 4-7 October, 2010

ABSTRACT

Reservoir simulations and monitoring of CO₂ storage require specific petrophysical data. We show and illustrate an integrated workflow dedicated to CO₂, including log data analysis and laboratory measurements.

This workflow has been applied on the Ketzin site. It is the first in-situ testing site of CO₂ injection in Germany and is located near the city of Ketzin. Carbon dioxide has been injected into a saline aquifer of the Triassic Stuttgart Formation in an anticlinal structure of the northeast German Basin. Two observation wells are used to detect the CO₂ plume arrival time, among other quantities, and all three wells are equipped with permanent resistivity sensors to monitor the change of the resistivity map during injection.

As clearly evidenced by NMR logs, the formation considered for injection contain a significant amount of clays. The cut-off for clay bound water has been determined precisely on two sub-regions using centrifuge data, in conjunction with experiments designed to obtain drainage capillary pressure.

For reservoir simulations, capillary pressure and relative permeability in drainage and imbibition are necessary. As a first step, we used air-brine centrifuge drainage capillary and water relative permeability curves, which can be used quickly in pre-simulations.

For monitoring purposes, formation factor, drainage and imbibition resistivity index curves are necessary. These data have been acquired using the Fast Resistivity Index Measurement method in drainage and imbibition.

Finally, the caprock has also been considered: pore diffusivity was determined using a quick NMR deuterium tracer technique, and permeability using an innovative technique.

Such a data set can be acquired in a reasonable amount of time and is very useful for the above mentioned aspects, especially as constraints for the evaluation of time-lapse results from the resistivity sensor array. Since similar data are acquired using different techniques (e.g. capillary pressure), this workflow also provides a consistency control in addition to standard quality control.

INTRODUCTION

Carbon Capture and Sequestration (CCS) is one of the many solutions to limit the current global warming. Although depleted oil and gas reservoirs can be used for CCS, their worldwide capacity and distribution is much less attracting than saline aquifer. From the petrophysical point of view, quick appraisal of such formation must be performed with appropriate workflow. These workflows are different from those applied to oil and gas reservoirs because first drainage is a key process. Also, we characterize caprock samples and this is only performed in gas storage situations.

Our workflow (Figure 1) begins at the logging data in order to select the appropriate samples representative of a given rock-type or characterized by different NMR pore structure (when NMR logs are available). In the present context, the amount of clay bound water is important and NMR logs were used for this purpose. Basic data such as porosity, water permeability and formation are first acquired on plug after coring and re-saturation. For the caprock zone, these basic data may not be easy to collect without appropriate techniques, as will be seen. Also, the CO_2 diffusivity information is collected for caprocks. Then the centrifuge technique can give rapidly capillary pressure curves and water relative permeability in first drainage on several samples. In the present situation, electrical properties were needed to calibrate a new in-situ electrical monitoring system. They can be measured either by centrifuge (CRIM method, [1]) or individually in specific cells. In the present situation, the samples were too fragile and only the individual measurements could be performed.

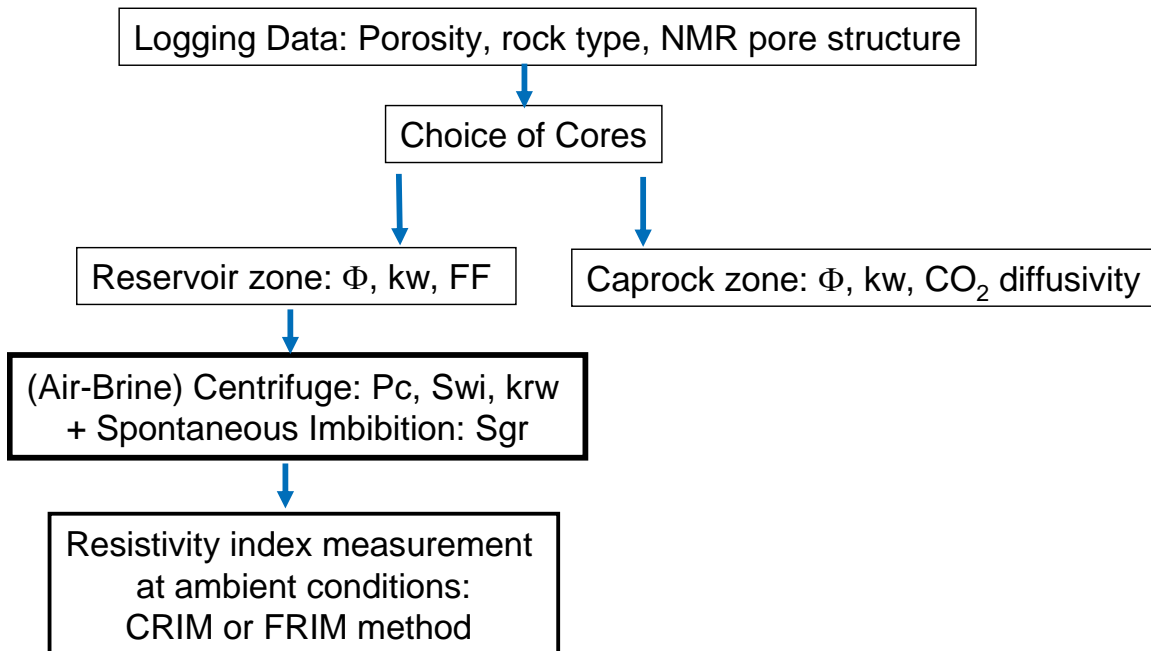


Figure 1: Workflow for the petrophysical measurements.

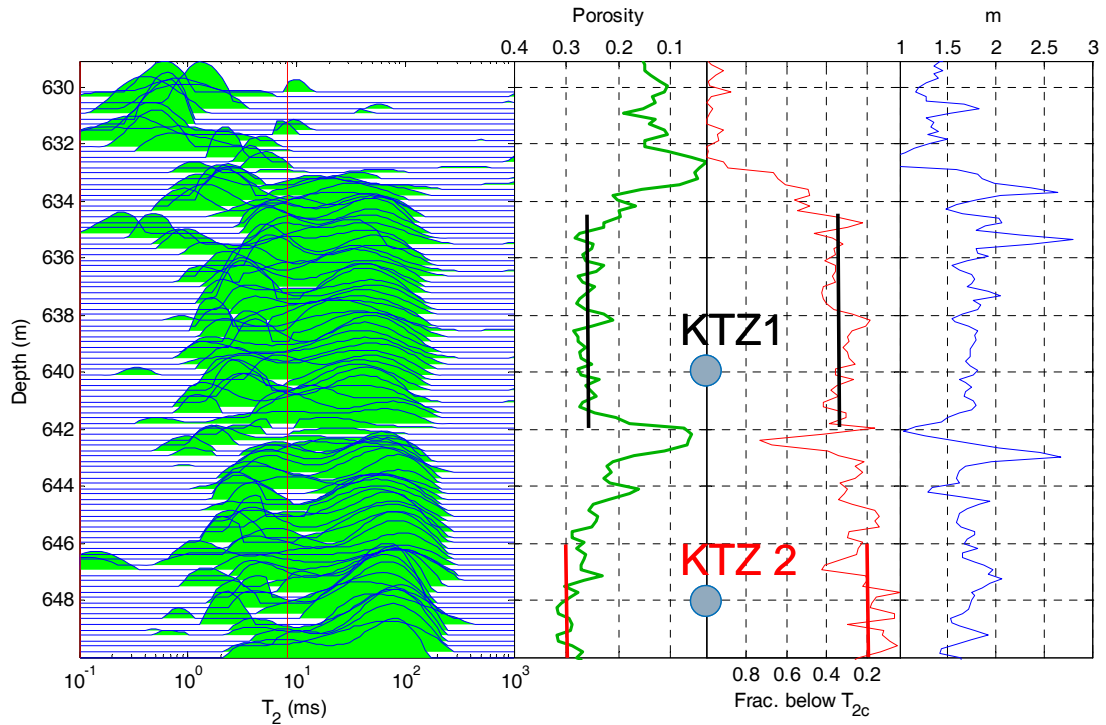


Figure 2: NMR and shallow resistivity log analysis of the reservoir zone giving porosity, clay content (fraction of porosity labeled fraction below T_{2c}) and cementation exponent m . The big circles indicate the location of the samples, and the vertical straight line indicate the T_2 cut-off used to calculate irreducible. The upper and lower zones are separated by a thin dense layer at 642 m.

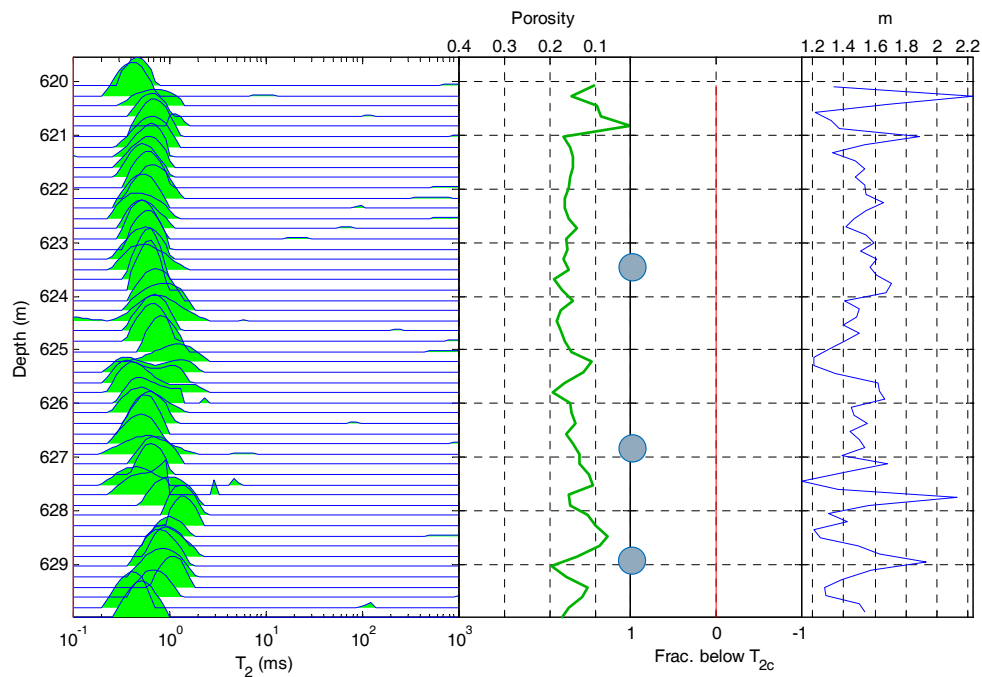


Figure 3: NMR and shallow resistivity log analysis for the caprock giving porosity and cementation exponent m . The big circles indicate the location of the samples.

Log data analysis and sample characterization

NMR and resistivity log data have been extracted from the Dlis file and analyzed (Figure 2, Figure 3). For NMR, we used the raw magnetization data and computed T_2 distributions using an in-house software at the highest possible vertical resolution (0.25 m). For resistivity, we extracted the shallow resistivity track (MCFL resistivity track reading in the "invaded zone"). Then, the cementation exponent m of the Archie relationship has been calculated from the relations $m = -\log(FR)/\log(\Phi)$ and $FR = R_t/R_w$ where R_t is the resistivity value given by the tool, R_w is the mud resistivity, and Φ is the NMR log porosity. Laboratory and log values are given in Table 1 and 2.

For the reservoir zone, clay bound water can be quantified using a cut-off of 8 ms, as a result of laboratory calibration (Figure 2). The cementation value m is roughly in globally with laboratory results. For the caprock zone, the porosities are uniform and significant (15 %, Figure 3) and the NMR pore size distribution shows only small fluctuations.

NMR laboratory data indicate similar T_2 distributions (Figure 4) at 100% saturation. For each sample, we adjusted the T_2 cut-off value for each sample in order to obtain the saturation value after centrifuge ($P_c \text{ max} = 2.2 \text{ bar}$). We found cut-off values between 5 and 9 ms. An average value of 8 ms was chosen in the log interpretation.

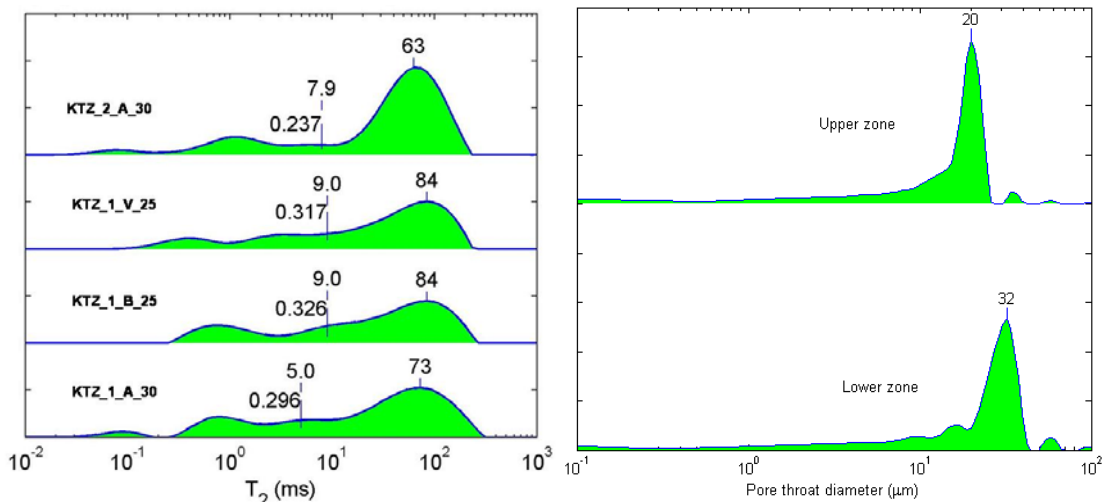


Figure 4: Left: NMR pore size distribution measured on different plugs from the upper (KTZ1) and lower zones (KTZ2). Numbers indicate the T_2 cut-off and the fraction of clay bound water (CBW) in order to obtain the measured saturation after centrifugation. An average value of 8 ms has been chosen in the log interpretation.

CBW is larger in the upper zone. Right: Mercury injection pore throat size distribution measured on sample KTZ 1c (upper zone) and KTZ 2b (lower zone). Note that the lower zone sample is less permeable, although the mode of the distribution is larger.

Centrifuge data and analysis: P_c and k_{rw}

In general, the centrifuge technique allows a quick and precise measurement of capillary pressure in drainage and forced imbibition, and an estimation of relative permeability curves in these cycles. In the case of air-brine fluid system which is the most appropriate

for CO₂-brine application, the very high mobility of the gas phase compared to the brine phase cannot be captured in the experiments. Hence, we obtain only the water relative permeability curve in drainage (the forced imbibition cycle is not useful here). Compared to the situation in which both the displaced and displacing phase Kr curves are determined (oil-water case with similar viscosity), the accuracy of the Krw curve in air-brine experiments is much better. The great advantage of centrifuge air-brine Kr experiments is that it is not subjected to fingering instabilities induced by local heterogeneities.

We performed centrifuge and relative permeability measurements using an automatic centrifuge described in Fleury et al. [2]. For capillary pressure, we used the Forbes method [3] to calculate capillary pressure curves from average saturation data. For relative permeability, we calculated the water relative permeability in the same multi-speed experiment using the Cydar software [4] from transient saturation data. At the end of drainage, samples are immersed in water in order to obtain the residual gas saturation. Prior to centrifugation, brine permeability and formation factor are measured. For various reasons (corrosion, salt precipitation), a diluted brine (50 gr/l) has been used. Although the system can handle up to 60 mm sample length, we used sample length of 25 mm or 30 mm (D=40 mm) in order to improve the accuracy at low capillary pressures. The accuracy of volume measurements is 0.05 cc, about 1 % of the pore volume.

Using the Cydar software (Cydarex), we simulated the air/brine primary drainage centrifuge experiment for the four samples; full experimental centrifuge speed table was used for the simulations. In order to reproduce the measured brine productions, capillary pressure and relative permeability curves were adjusted through a two steps optimization process. First, starting from the Forbes solution for capillary pressures (Figure 4.2) and using relative permeability curves simply described by Corey's equations with exponents 1, capillary pressure curves were adjusted so that the simulated production matches the volume production at the end of each centrifuge speed step. Then, the relative permeability curves were adjusted in order to reproduce for each step the transient part of the production (Figure 4.3d). To smooth the curve, we used the analytical formulation (LET functions) given by Lomeland [5, 6] and simulated again the data.

We observe two groups of capillary pressure curves (Figure 5) corresponding respectively to the lower and upper zones of the reservoir. Adjusted capillary pressure curves remain close to the initial analytical Forbes solutions. The upper zone samples, less porous and more permeable, present a slightly higher entry pressure (>100mbar) and a higher irreducible water saturation (about 30%, Table 3) while the lower zone sample, has an entry pressure less than 100mbar and an irreducible water saturation about 24%.

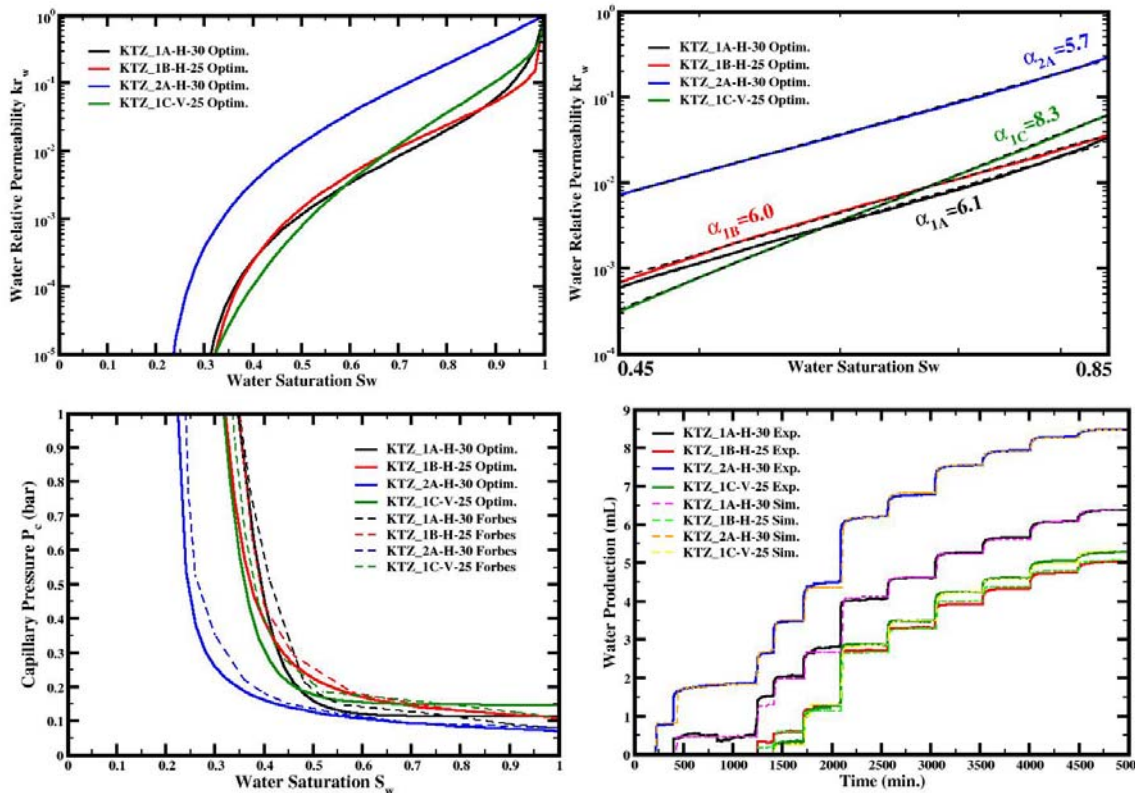


Figure 5: Water relative permeability curves from centrifuge experiment. Top left: best fit curves for the 4 samples; top right: zoom showing the slope in log-log scale; down left: P_c curves used for the K_r calculation and calculated using the Forbes method; down right: fitted and measured production curves

We observe two groups of water relative permeability curves as well (Figure 5), corresponding also to the two reservoir zones. For both zones, during the drainage process, water relative permeabilities decrease rapidly with water saturation. During early drainage ($S_w > 90\%$), water relative permeabilities of upper zone samples drop rapidly by a factor of ten. Then, in the intermediate saturation range (S_w between 0.85-0.45), all water relative permeabilities follow power law evolutions (Corey's relations) with high exponents (Figure 5), in agreement with the known range of values for gas-liquid first drainage [7]; horizontal samples from lower and upper zones present both exponents of the order of 6 (Figure 5). For the intermediate saturations, the less permeable sample, from the lower zone, has the highest water relative permeability, about one order of magnitude greater than the upper zone ones. Therefore, the apparent water permeability is 3 to 5 times higher for the less permeable sample of the lower zone. Water relative permeability of the vertical sample from the upper zone, follow a power law as well in the intermediate saturation range, with an exponent slightly greater than 8 (Figure 5).

From the point of view of apparent permeabilities of the two intervals studied, the relative permeability effects can easily compensate the difference of absolute permeabilities. We observe that in the water saturation range greater than 45%, water relative permeabilities are greater than 10^{-3} - 10^{-2} meaning that the apparent water

permeabilities will remain greater than 100 μ D-1mD. In such a case CO₂ injection can still be considered, but it will require more and more pressure as water saturation decreases in the reservoir. Below water saturations of 45%, relative water permeabilities drop drastically; thus water mobility will become too low and further increase of CO₂ saturation will not be possible in practice; consequently a significant part of the estimated reservoir volume will not be accessible for CO₂ storage.

Resistivity measurements: FF and RI

The formation factor has been measured using a classical face to face two electrode system, simultaneously with permeability. The measurement frequency is 1 kHz and we varied the brine salinity in some experiments. The formation brine composition is given in Table 4.

In clay rich systems, there is a well known excess conductivity due to double layer effects in the clays. This is usually studied by decreasing the salinity of the brine and plotting the conductivity of the sample vs. brine conductivity (Figure 6). The excess clay conductivity is given by the intercept at x=0 of the sample conductivity. The data can be fitted with the following best fit equation:

$$C_0 = 0.1119C_w + 0.0878 \text{ [S/m]} \quad R^2=0.999 \quad (1)$$

We see in the present situation that this offset is quite small. The formation factor calculation could be improved slightly using a Waxman-Smiths model in which the sample conductivity C_0 and formation factor FF are related by:

$$C_0 = \frac{1}{FF} (0.785 + C_w) \text{ in units of [S/m]} \quad (2)$$

instead of calculating $FF=C_0/C_w$.

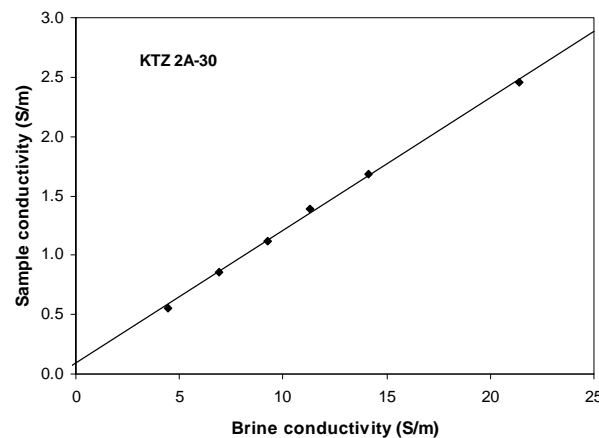


Figure 6: Sample conductivity versus brine conductivity using the formation brine composition.

The method used to measure resistivity index is the Fast Resistivity Index Measurement method called FRIM [8]. We measured resistivity indexes in drainage and spontaneous imbibition. In drainage, the pressure difference between air and brine has been increased gradually (typically 50, 100, 180, 360, 640, 1300, 1800 mBar) to decrease the saturation. We obtain a few points of the capillary curve (at the different pressure steps), and a "continuous" resistivity index curve which is insensitive to the choice or the number of pressure steps. In imbibition, the pressure difference is also decreased gradually.

In addition to the standard 1 kHz frequency measurement, the system allows scanning the frequency range [1 Hz – 1MHz] using a Solartron impedance meter [9]. This is of interest to study the low frequency range around 1 Hz, close to those used in the VERA monitoring system. These measurements are not described in this paper but we concluded that the resistivity index results at 1 kHz can be applied at 1 Hz.

The resistivity index curves on a sample from the upper zone is shown in Figure 7. It cannot be described by a simple Archie law. Indeed, there is first a sharp increase of RI at the beginning of drainage ($S_w^{-3.5}$), followed by a change of slope and a more classical behaviour ($S_w^{-2.0}$). The model deduced from the data is the following:

$$RI = S_w^{-3.5} \quad 0.82 < S_w < 1 \quad (3)$$

$$RI - RI_0 = S_w^{-2.0} \quad S_w < 0.82 \quad RI_0 = 0.56 \quad \text{in drainage and imbibition}$$

It means that the resistivity changes are larger at large saturation ($S_w \approx 0.8$) compared to a simple Archie law S_w^{-2} . The origin of the sharp increase at the beginning is not due to an experimental artefact (there is no dead volume correction and the RI curve is obtained directly from the data). A possible explanation is that a network of large pores may exist in the sample. This network may have a large contribution in terms of conductivity and when invaded by air, this contribution is rapidly lost. There is no hysteresis effects (no difference between drainage and imbibition) as expected for this type of porous media. For the sample of the lower zone, a lower saturation exponent is observed ($n=1.7$).

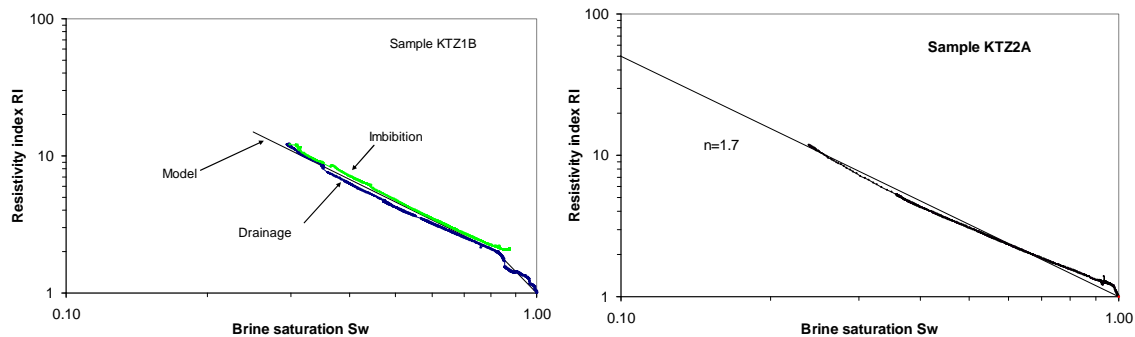


Figure 7: N₂-brine resistivity index measured at ambient conditions for sample KTZ1 (upper zone) and KTZ2 (lower zone). Note the small residual gas saturation for KTZ1.

Specific measurements on caprocks

Specific techniques must be used to characterize caprocks. The most important characterization is water permeability, and it may be time consuming or practically impossible using classical techniques. A second aspect concerns water diffusivity which gives a maximum diffusivity value of dissolved CO₂ in water. This is useful to simulate the slow migration of CO₂ at the top of the reservoir into the caprock for long periods of time.

For permeability, we used the method described in more details in [10]. When applying a pressure gradient across a sample, the displaced volume of water is measured on both sides with high precision pumps ("push-pull" mode as shown in Figure 8). At steady state it would correspond to the volume pushed from inlet to outlet. Hence, when the evolution is linear, the slopes corresponding to the upstream and downstream water flow can be gathered. Then the successive flow rates (Q) are plotted against the pressure gradient (P_u-P_d) (Figure 8). The three points obtained align along a slope proportional to the permeability. An average permeability of 27.4 nD was estimated from this slope. Note that the measurement time is about 9 hours, a reasonable time for such low permeability. However, this duration does not include the time needed to re-saturate at 100 % the sample when it is not well preserved. Note also that samples are never dried and we measured porosities using NMR. The orientation of the plug is such that the measurement represents a horizontal permeability.

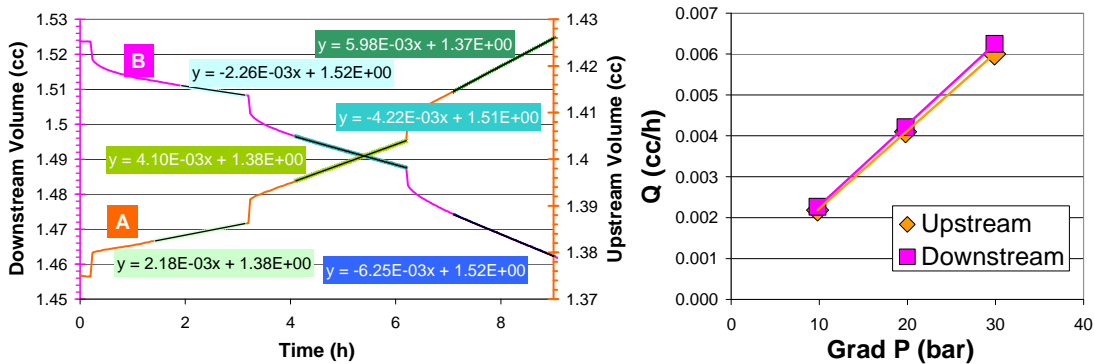


Figure 8: Measurement of the piston strokes during "push-pull" permeability experiments (left). Resulting flow rate vs. pressure gradient (right) yielding a water permeability of 29 nD.

Diffusion data are useful for the simulation of long term CO₂ migration into the caprock. We measured the pore water diffusivity that can be used as an upper limit of the diffusivity of dissolved CO₂ in the caprock. The method used is described in Fleury et al. [11] and Berne et al. [12] in more details. Essentially, a small sample (e.g. a cube of size 10 mm) initially saturated with brine is immersed in deuterium D₂O (purity 99.5%). Because D₂O (²H) has a very different resonance frequency (in our case 3.6 MHz instead of 23.7 MHz) and is therefore not measured, we can measure a ¹H water concentration inside the sample as a function of time by simply recording the magnetization as a function of time. The corresponding T₂ distributions are shown in Figure 9 for 3 different

diffusion times: water diffusing outside the sample is characterized by a long relaxation time and can be separated from the water inside the sample. Hence we can obtain the concentration as a function of time (Figure 9). Using an analytical expression of the diffusion in a cube [12], we deduce the pore diffusivity from the normalized concentration vs. time. The fitted pore diffusivity D_p is $0.8 \times 10^{-9} \text{ m}^2/\text{s}$ at 30°C while the bulk water diffusivity at the same temperature is $2.6 \times 10^{-9} \text{ m}^2/\text{s}$. This result is also coherent with a value of cementation m of 1.77, close to the value computed in the log (Figure 3).

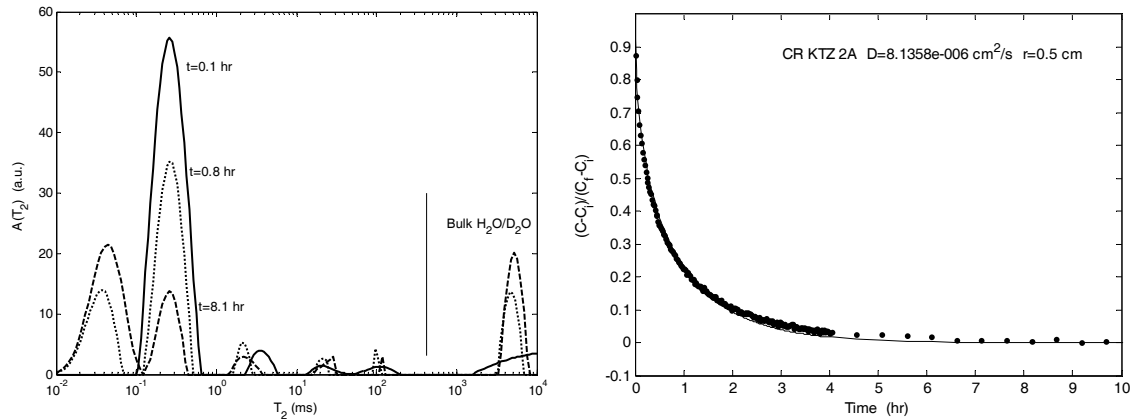


Figure 9: T_2 distribution at different times in the D_2O diffusion experiment. Caprock sample CR KTZ2A, porosity 0.21 (left). The fitting of the concentration curve (directly deduce from the NMR magnetization) using a diffusion model in a cube yields a diffusion coefficient of $8.1 \cdot 10^{-6} \text{ cm}^2/\text{s}$ at 30°C .

CONCLUSION

Several transport properties have been evaluated on reservoir and caprock samples from the Ketzin site, well 201. On reservoir samples, we evaluated, beside water permeability, porosity and clay content, electrical, capillary and relative permeability properties. These properties are useful for the interpretation of resistivity monitoring, and the prediction of CO_2 invasion and saturation during injection. For the caprock zone, we evaluated water permeability and water diffusivity, useful for the prediction of CO_2 migration into the caprock. The log analysis performed on the same well was useful to extend the results obtained on different samples to specific intervals.

Capillary pressure measurements indicate that the smallest saturation that can be reached is about 20% for the lower zone, and 28 % for the upper reservoir zone. For the upper zone, both relative permeability and resistivity curves present a peculiar behaviour in the saturation range above 0.8, i.e. a sharp increase of resistivity and a sharp decrease of relative water permeability compared to usual behaviour. This is not observed on the lower zone in which more standard behaviour is observed. The two different behaviour is most likely linked to the different clay amount and distribution as observed on CT scans and NMR. For resistivity, typical m and n values are close to 1.5.

For the caprock zone, we found a water permeability of 29 nD ($29 \cdot 10^{-21} \text{ m}^2$) instead of much larger values previously published. This is due partly to the difficulty of preparing and handling non preserved argillaceous caprock samples. Indeed, on one sample, the presence of visible fractures yielded permeability values in the range of mD. Water diffusivity values measured by NMR techniques gave the expected values. It can be used as an upper limit for the diffusivity of dissolved CO_2 in water.

ACKNOWLEDGEMENTS

We thank the French National Research Agency (ANR) for supporting this work. P. Poulain, F. Norrant and Y. Larabi contributed also to the experimental program.

REFERENCES

- 1 Han M., M. Fleury and P. Levitz, Effect of the pore structure on resistivity index curves, International Symposium of the Society of Core Analysts, Calgary, Canada, 10-13 September, 2007.
- 2 Fleury M., P. Poulain and G. Ringot, 'A capacitance technique for measuring production while centrifuging', Proceedings of the International Symposium of the Society of Core Analysts, La Haye, September 14-16, 1998.
- 3 Forbes, P.L., 1991, Simple and Accurate Methods for Converting Centrifuge Data into Drainage and Imbibition Capillary Pressure Curves, SCA paper 9107 presented at The Society of Core Analysts Annual Technical Conference, San Antonio, Texas, August 21-22.
- 4 Cydar , Design and interpretation of petrophysical experiments, 2010, Cydarex company (www.cydarex.fr).
- 5 Lomeland F., Ebeltoft E. and Hammervold Thomas W.: "A New Versatile Relative Permeability Correlation", SCA 2005-32.
- 6 Lomeland F. and Ebeltoft E. : "A New Versatile Capillary Pressure Correlation", SCA 2008-8.
- 7 Honarpour M., Koederitz L., Harvey A.H., Relative permeability of Petroleum Reservoir, CRC Press, Boca Raton, florida, 1986.
- 8 Fleury M., 'FRIM: a Fast Resistivity Index Measurement Method', Proceedings of the International Symposium of the Society of Core Analysts, La Haye, September 14-16, 1998.
- 9 Fleury M. and F. Liu, Frequency effect on resistivity index curves using a new method, Proceedings of the 41st Annual SPWLA Symposium, Dallas, June 4-7 2000.
- 10 Boulon, P.F., Bretonnier, P., Gland N., J.M. Lombard, Low permeability measurements with water on clay sample. Contribution of steady state method compared to transient methods, SCA 2010 Symposium, Halifax, Canada, October, 2010.
- 11 Fleury M., P. Berne, P. Bachaud, Diffusion of dissolved CO_2 in caprock. Energy Procedia 1 (2009) 3461–3468.
- 12 Berne Ph., P. Bachaud, M. Fleury, Diffusion properties of carbonated caprocks from the Paris Basin, OGST Special Issue, 2010, Available at ww.ogst.fr.

Table 1: Main characteristics of the samples from the reservoir zone.

Sample	Depth (m)	Porosity (%)		Water Permeability	Clay bound water (%)	
		lab	log		lab.	log
KTZ 1	639.7	26.8 - 28	28	182 - 280	30 - 32	35
KTZ 2	648.9	31.4	30	104	24	20

Table 2: Main characteristics of the samples from the caprock zone.

Sample	Depth (m)	Porosity (%)		Permeability (nD)
		lab	log	
CR KTZ 1	623.6	14	17	29
CR KTZ 2	626.8	20.3 – 21.1	15	-
CR KTZ 3	629.4	18.8 – 22.5	19	-

Table 3: Summary of the results for the reservoir samples. Porosity, water permeability, irreducible water saturation after centrifuge and residual gas saturation after spontaneous imbibition.

Sample	Φ (%)	Kw (mD) KTZ Brine	FF – m KTZ Brine	Swirr drainage (%)	Sgr imbibition (%)
KTZ-1A-H	28.0	182	11.4 - 1.81	30	10.0
KTZ-1C-V	28.0	238	11.9 - 1.90	32	10.7
KTZ-1B-H	26.8	280	11.4 - 1.80	32	11.1
KTZ-2A-H	31.4	104	8.6 – 1.89	24	18.3

Table 4: Formation water composition

Species	Concentrations (gr/l)
Cl	141.8
S	4.082
Na	86.52
K	0.462
Ca	2.186
Mg	0.804
Sr	0.0638
Ba	0.0009
Total	235.9187